ResearchGate

See discussions, stats, and author profiles for this publication at: https://www.researchgate.net/publication/309181600

Transport of dilute organics through dense membranes: Assessing impact on membrane–solute interactions

Article *in* Journal of Membrane Science · February 2017

DOI: 10.1016/j.memsci.2016.10.013

CITATIONS
6

READS
239

5 authors, including:

Sofia Fraga
REQUIMTE
5 PUBLICATIONS **32** CITATIONS
SEE PROFILE

Anna Kujawska
Nicolaus Copernicus University
23 PUBLICATIONS **480** CITATIONS
SEE PROFILE

Wojciech Kujawski
Nicolaus Copernicus University
184 PUBLICATIONS **3,382** CITATIONS
SEE PROFILE

Carla Brazinha
LAQV, REQUIMTE, FCT, Universidade Nova de Lisboa
36 PUBLICATIONS **329** CITATIONS
SEE PROFILE

Some of the authors of this publication are also working on these related projects:

[M3-S Conference] Membrane materials - modification and separation View project

Project of Fundação para a Ciência e a Tecnologia, Portugal View project

All content following this page was uploaded by Carla Brazinha on 20 February 2018.

The user has requested enhancement of the downloaded file.

Journal of Membrane Science 523 (2017) 346–354

Contents lists available at ScienceDirect

Journal of Membrane Science

journal homepage: www.elsevier.com/locate/memsci

Transport of dilute organics through dense membranes: Assessing impact on membrane-solute interactions

Sofia C. Fraga[a], Anna Kujawska[b], Wojciech Kujawski[b,*], Carla Brazinha[a,**], João G. Crespo[a]

[a] LAQV/Requimte, Faculdade de Ciências e Tecnologia, Universidade Nova de Lisboa, Campus de Caparica, 2829-516 Caparica, Portugal
[b] Faculty of Chemistry, Nicolaus Copernicus University in Torun, 7 Gagarina Str., 87-100 Torun, Poland

ARTICLE INFO

Keywords:
Mass spectrometry
Pervaporation
On-line monitoring
Time-dependent diffusion coefficients
Solute solubilisation

ABSTRACT

Polydimethylsiloxane (PDMS) membranes were synthesised by varying the degree of crosslinking and were characterised in a pervaporation system coupled to a mass spectrometry (MS) for on-line monitoring and collecting data points with an interval of 2 s. This monitoring approach allows obtaining very precise information about the impact of solutes' solubilisation within the membrane and their influence on solvent permeation. Using dilute aqueous solutions of ethyl acetate and hexyl acetate, it is shown how solutes with diverse nature and diverse partitioning into the membrane, determine the transport of solvent and solute by progressively modifying the membrane transport properties. From the evolvement of the time-dependent diffusion coefficients of the selected solutes during transient transport, it is possible to infer about solute-membrane molecular interactions and their impact in terms of membrane rearrangement and fluidification.

1. Introduction

The degree of crosslinking of a polymeric membrane may determine its physicochemical properties: a higher degree of crosslinking leads to a more rigid polymer and, contrarily, a lower degree of crosslinking leads to a more flexible polymer network [1]. Polydimethylsiloxane, PDMS, is a silicone-based polymer widely used in different areas of separation processes [2], e.g. gas separation and hydrophobic pervaporation for the selective transport of organics from water [3–6]. The permeation of a solute through PDMS is commonly described by the solution-diffusion model, which is based on solute-polymer interactions [7]. These interactions may be important in pervaporation processes, especially when the permeating species have high affinity to the membrane causing alterations in its structure, which impact the properties of solute transport in a structure-transport relationship [8]. These modifications in the membrane structure and, consequently in the membrane properties, may be particularly noticeable during the transient state of the permeation process. Indeed, the membrane is dry in the first instants of permeation and then it shows a progressive solubilisation of solute within its structure with time. This increase of local solute concentration inside the membrane may lead to a rearrangement of the membrane polymeric matrix. Namely, a fluidification of the membrane may occur, leading to a faster transport of solutes, which may be quantified by an increase of the concentration-dependent diffusion coefficients of solutes as in [9] or, as in our previous work [10], by an increase of the time-dependent diffusion coefficient of solutes. Therefore, the study and estimation of the transport properties and, in particular, the time-dependent diffusion coefficients of solutes, in the whole transient period, is a key factor for a better understanding of the membrane internal structure rearrange-

Abbreviations: $c_{i,bulk}$, concentrations of the solute *i* in the bulk (-); $c_{i,bl}$, concentrations of the solute *i* in the boundary layer (-); c_{im}^{perm}, concentrations of the solute *i* in the membrane in the permeate (-); c_i^{perm}, concentrations of the solute *i* in the permeate (-); $c_{i,m}^*$, equilibrium concentration in the membrane (wt./wt.); $c_{i,f}^*$, equilibrium concentration in the liquid (wt./wt.); D_{i-j}, diffusion coefficient of the solute in the solvent calculated using the Wilke-Chang equation ($m^2\ s^{-1}$); D_i, diffusion coefficient of the solute *i* ($m^2\ s^{-1}$); D_it, time-dependent diffusion coefficient($m^2\ s^{-1}$); Dt=∞, diffusion coefficient of compound *i* at the steady state ($m^2\ s^{-1}$); EF -, enrichment factor; EtAc, ethyl acetate; HxAc, hexyl acetate; H_i, Henry's law coefficient (Pa^{-1}); I_it, electrical signal intensity of the compound *i* in the instant *t* [A]; $I_it=\infty$, electrical signal intensity of the compound i at the steady state (t=∞) $J_{i,bl}$, flux across the boundary layer ($m^{-3}\ m^{-2}\ s^{-1}$); $J_{i,m}$, flux across the membrane ($m^{-3}\ m^{-2}\ s^{-1}$); $J_{i,ov}$, overall flux ($m^{-3}\ m^{-2}\ s^{-1}$); J_i, partial flux of the compound i ($m^{-3}\ m^{-2}\ s^{-1}$); J_T, the total flux ($m^{-3}\ m^{-2}\ s^{-1}$); Jit=∞, partial flux in the steady state ($m^{-3}\ m^{-2}\ s^{-1}$); $k_{i,bl}$, boundary layer mass transfer coefficient ($m\ s^{-1}$); $k_{i,ov}$, overall mass transfer coefficient ($m\ s^{-1}$); $k_{i,m}$, membrane mass transfer coefficient ($m\ s^{-1}$); z_{bl}, boundary layer thickness (m); L, thickness of the membrane (m); P, permeability of a solute i ($m^2\ s^{-1}$); P_i^G, gas-phase permeability of compound i. ($m^2\ s^{-1}$ Pa); p_{ifeed}, partial pressure of compound *i* in the feed liquid; Re_R, Reynolds number at the outer radius of the cell; S_i, sorption coefficient of compound *i*(-); S_i^L, liquid-phase sorption coefficient (-); S_i^G, gas-phase sorption coefficient (Pa^{-1}); $w_{i,permeate}$, permeate weight fraction; $w_{i,feed}$, feed weigh fraction; α_{i-j}, selectivity of the solute *i* in relation to the solvent (-); β_i, enrichment factor of the pervaporation process of solute *i* (-)

* Corresponding author. Tel.: +48 56 611 4315.
** Corresponding author. Tel.: +351 21 294 83 85.
E-mail addresses: kujawski@chem.umk.pl (W. Kujawski), c.brazinha@fct.unl.pt (C. Brazinha).

http://dx.doi.org/10.1016/j.memsci.2016.10.013
Received 15 April 2016; Received in revised form 7 September 2016; Accepted 9 October 2016
Available online 11 October 2016
0376-7388/ © 2016 Elsevier B.V. All rights reserved.

ment when solutes permeate through [10].

Previous works [10–13] proved that Mass Spectrometry (MS) is a suitable tool for monitoring of pervaporation systems with binary or multicomponent solutions in the feed stream. MS is able to follow the transport of each species present in the feed solution to the permeate side, following and characterising the permeation of the whole operation period (transient and steady-state regimes) of mixtures of compounds through dense films. Therefore, permeate partial pressures and composition, fluxes, and solutes' selectivities and diffusivities may be measured on-line with a time interval of two seconds or less if intended (depending on the number of compounds followed) [10]. Design and fabrication of new materials can directly benefit from this study. Applying this methodology of characterisation of mass transport through dense membranes [10], solutes with different molecular mass and affinity to the membranes' may be selected, in order to understand their impact on the membrane structure and transport behaviour.

The separation of organic compounds from aqueous media by hydrophobic pervaporation is commonly subject to mass transfer limitations in the liquid boundary layer adjacent to the membrane, leading to concentration polarisation effects. Schäfer et al. [14] determined the degree of concentration polarisation of aroma compounds in pervaporation experiments as a function of the cross-flow velocity over a membrane with a hydrophobic top-layer relatively thin. The author concluded that compounds with a high sorption coefficient into the membrane polymer, such as hexyl acetate, were strongly affected by concentration polarisation compared to those with low sorption coefficient. Baker et al. [15] demonstrated that this phenomenon can be overcome using thick silicone rubber membranes (more than 20 μm). In this case, the permeation of organic compounds is controlled by the transport across the membrane, which dominates over the transport across the stagnant boundary layer. Similarly, thick PDMS membranes were prepared in this work (much thicker than 20 μm) and used in order to prevent concentration polarisation effects, allowing for a more detailed interpretation of the mass transport mechanisms of the solute transport across the membranes under study.

In this work the impact of various operating conditions, involved in the permeation of dilute organic solutes, on potential rearrangements of the polymeric membrane, was assessed. The effect of these operating conditions was evaluated by measuring the solvent (water) flux (expected to be constant when the structure of the membrane remains constant), and by measuring the solutes' transport properties at steady state (diffusion coefficients and selectivities) and during the transient regime (time-dependent diffusivities), using on-line MS as a monitoring tool. Time-dependent diffusion coefficients, D(t), were calculated, from the initial transient period until steady state was reached. Based on these values it is possible to conclude about the relevance of solute–membrane interactions and rearrangement of the membrane structure due to the presence of permanent solutes.

2. Theoretical concepts

2.1. Mass transport in the feed boundary layer

In pervaporation, the feed-side concentration polarisation phenomena may be severe especially in the presence of solutes, such as hexyl acetate, with high affinity to the PDMS membrane material. This phenomenon represents a mass resistance to the solute transport, due to the fact that the transport of the solute in the feed boundary layer towards the membrane is not fast enough to compensate the sorption of the solute occurring at the upstream surface of the membrane [14,15]. Consequently, the solute concentration in the boundary layer decreases and, thus, its driving force and flux decrease as well. The model most commonly used to describe this phenomenon is the thin film model where it is assumed a stagnant boundary layer adjacent to the membrane [14,15], as shown in Fig. 1, in which the solute transport is diffusive rather than convective.

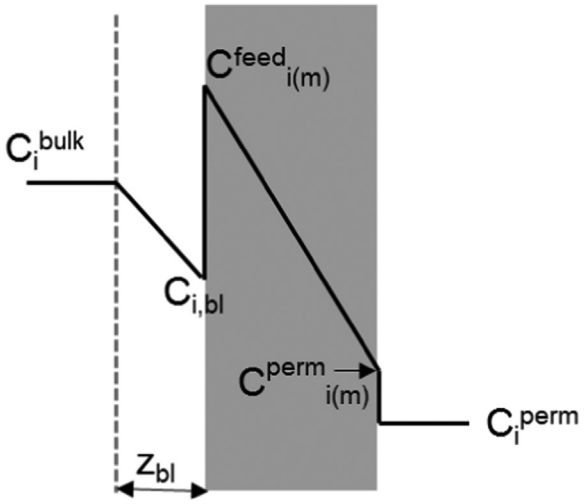

Fig. 1. Representation of solute concentration profile in a pervaporation process, adapted from [14].

At steady state, assuming Fickian diffusion across both boundary layer and membrane, the flux across the boundary layer, $J_{i,\ bl}$, and across the membrane, $J_{i,m}$, are equal yielding a defined overall flux, $J_{i,\ ov}$, such that $J_{i,\ bl} = J_{i,m}, = J_{i,\ ov}$ ($m^3\ m^{-2}\ s^{-1}$) [14].

$$J_{i,bl}=k_{i,bl}\,[c_{i,bulk}-c_{i,bl}] \tag{1}$$

$$J_{i,m}=k_{i,m}S_i^L\,[c_{i,bl}-c_{i(m)}^{perm}] \tag{2}$$

$$J_{i,ov}=k_{i,ov}\,[c_{i,bulk}-c_i^{perm}] \tag{3}$$

where $k_{i,\ bl}$ ($m\ s^{-1}$) is the boundary layer mass transfer coefficient; $k_{i,m}$ (m/s) the membrane mass transfer coefficient; $k_{i,\ ov}$ (m/s) the overall mass transfer coefficient and $c_{i,\ bulk}$, $c_{i,\ bl}$, c_i^{perm} (-) are the concentrations of the solute *i* in the bulk, in the liquid boundary layer and in the permeate respectively. S_i^L(-) is the liquid-phase sorption coefficient of the solute *i* and z_{bl} (m) is the boundary layer thickness. The "resistance in series model" is obtained in Eq. (4), combining Eqs. (1)–(3) and assuming vacuum conditions in the downstream side of the membrane, which allows to consider the solute concentration in permeate negligible:

$$\frac{1}{k_{i,ov}}=\frac{1}{k_{i,bl}}+\frac{1}{k_{i,m}S_i} \tag{4}$$

The concentration polarisation phenomena in an aqueous phase, in a cell with radial flow was determined by Urtiaga et al. [16]. Particularly, a correlation was developed to calculate the boundary layer mass transfer coefficient [16] in a cell similar to the one used in this work:

$$k_{bl}=131.\ 2Re_R^{0.5}\,Sc^{0.33}D \tag{5}$$

where D_{ij} ($m^2\ s^{-1}$) is the diffusion coefficient of the solute *i* in the solvent *j* calculated using the Wilke-Chang equation [17]. The feed boundary layer thickness z_{bl} (m) was calculated as the ratio of the boundary layer mass transfer coefficient $k_{i,\ bl}$ (m/s) and $D_{i\text{-}j}$ ($m^2\ s^{-1}$) given by

$$k_{bl}=\frac{D_{ij}}{z_{bl}} \tag{6}$$

Re_R is the Reynolds number at the feed side of the cell given by

$$Re_R=\frac{F\rho}{\pi\mu R} \tag{7}$$

where F ($m^3\ s^{-1}$) is the volumetric flow rate of the feed, ρ ($kg\ m^{-3}$) the density, μ ($kg\ m^{-1}\ s^{-1}$) the viscosity and R (m) the radius of the cell. Combining, Eq. (4) and Eq. (5):

$$\frac{1}{k_{i,ov}}=\frac{1}{131.\ 2xRe_R^{0.5}Sc^{0.33}D_{i-j}}+\frac{1}{k_{i,m}S_i} \quad (8)$$

Eq. (8) may assess whether concentration polarisation phenomenon is relevant in a particular overall transport of solute. In this case, the term related to the mass resistance of the transport of solute across the liquid boundary layer, $\frac{1}{131.2xRe_R^{0.5}Sc^{0.33}D_{i-j}}$, is comparable or higher than the term related to the mass resistance of the transport of solute across the membrane, $\frac{1}{k_{i,m}S_i}$.

2.2. Steady-state transport

The flux of a solute i at steady state, assuming a Fickian diffusion (1st Fick's law), is expressed as

$$J_i=\frac{D_i}{L}\times(c_{i(m)}^{feed}-c_{i(m)}^{perm}) \quad (9)$$

The permeability of a solute *i* at steady state may be calculated, from a modification of Eq. (2), as reported by Baker et al. [7]:

$$J_i=\frac{P_i}{L}\times(c_i^{feed}-c_i^{perm}) \quad (10)$$

where P_i (m^2/s) is the (liquid-phase) permeability of solute *i* and L (m) is the thickness of the membrane. The diffusion coefficient D_i (m^2/s) under steady state is calculated by the sorption-diffusion model, and using the sorption coefficient of compound *i* experimentally obtained, as follows:

$$P_i=S_i\times D_i \quad (11)$$

At the liquid solution/membrane feed interface, considering equal chemical potentials on either side (interfacial equilibrium), the concentration is given by:

$$c_{i(m)}^{feed}=\frac{\gamma_i^{feed}c_i^{feed}}{\gamma_{i(m)}^{feed}}=S_i^L\times c_i^{feed} \quad (12)$$

where S_i^L(-) is the liquid-phase sorption coefficient. The equivalent expression for the permeate side is given by:

$$c_{i(m)}^{perm}=\frac{\gamma_i^{perm}}{\gamma_{i(m)}^{perm}}\times\frac{p_i^{perm}}{p_i^{sat}}=S_i^G\times p_i^{perm} \quad (13)$$

where S_i^G(Pa^{-1}) is the gas-phase sorption coefficient. The feed and permeate concentrations in the membrane, respectively $c_{i(m)}^{feed}$ and $c_{i(m)}^{perm}$, can be substituted in the Fick's law Eq. (10) respectively as a function of p_i^{feed} and p_i^{perm}. However, the feed sorption coefficient is a liquid-phase sorption coefficient, S_i^L(-), and the permeate sorption coefficient is a gas-phase sorption coefficient, S_i^G (Pa^{-1}). These two factors can be combined considering a hypothetical vapour in the equilibrium with the liquid, what can be written as follows:

$$c_i^{feed}=\frac{\gamma_i^{feed,G}}{\gamma_i^{feed,L}p_i^{sat}}p_i^{feed}=\frac{S_i^L}{H_i}p_i^{feed} \quad (14)$$

where p_i^{feed} is the partial pressure of compound *i* in the feed liquid and the term $\gamma_i^{feed,L}.p_i^{sat}/\gamma_i^{feed,G}$ is the Henry's law coefficient, H_i (Pa^{-1}). The liquid-phase and gas-phase sorption coefficients, respectively S_i^L and S_i^G relates as

$$S_i^L=S_i^G H_i \quad (15)$$

Therefore, the feed concentrations in the membrane, $c_{i(m)}^{feed}$, may be calculated combining Eqs. (12) and (14)

$$c_{i(m)}^{feed}=\frac{S_i^L}{H_i}\times p_i^{feed}=S_i^G\times p_i^{feed} \quad (16)$$

From Eq. (10) and using Eq. (14) and the definition of the Henry's law coefficient we obtain:

$$J_i=\frac{P_i^G}{L}\times(p_i^{feed}-p_i^{perm}) \quad (17)$$

$$J_i=\frac{P_i^G}{L}\times\left(\frac{c_i^{feed}\gamma_i^{feed,L}p_i^{sat}}{\gamma_i^{feed,G}}-p_i^{perm}\right) \quad (18)$$

$$J_i=\frac{P_i^G}{L}\times(c_i^{feed}H_i-p_i^{perm}) \quad (19)$$

where P_i^G ($m^2\ s^{-1}\ Pa^{-1}$) is the gas-phase permeability of compound *i*, which is the product of gas-phase sorption coefficient S_i^G and the diffusion coefficient D_i.

Therefore, permeability of solute *i*, P_i (m^2/s), is calculated for systems at steady-state, using the sorption coefficient of compound *i* experimentally obtained, as in

$$J_i=\frac{P_i}{L}\times\left(c_i^{feed}-\frac{c_i^{perm}}{H_i}\right) \quad (20)$$

The selectivity of the solute *i* (ethyl acetate or hexyl acetate) in relation to the solvent *j* (water), $\alpha_{i\text{-}j}$ (-), corresponds to the ratio of the solute and the solvent permeabilities, $P_{solute}/P_{solvent}$, and the enrichment factor of the pervaporation process of solute *i*, EF (-) [18], is the ratio between the permeate weight fraction, $w_i^{permeate}$ and the feed weigh fraction, w_i^{feed}, $w_i^{permeate}/w_i^{feed}$.

2.3. Transient transport

The transient transport of solute *i* (ethyl acetate and hexyl acetate) through PDMS membrane was monitored by online mass spectrometry and characterised in terms of its flux using Eqs. (21)–(23).

The partial flux of the compound *i* under steady-state, J_i (t=∞) (m s^{-1}) is calculated multiplying the total flux, J_T (m s^{-1}), obtained through the condensed vapours in the trap, by the solute concentration, $[i]_{perm,(t=\infty)}$, (-) in the permeate in the steady state given by the MS. The solute concentration is calculated as the ratio between the solute partial pressure and the total pressure under steady-state, as described elsewhere [10].

$$J_i(t=\infty)=J_T\times[i]_{perm(t=\infty)} \quad (21)$$

Considering the linear relation between the fluxes and the corresponding electrical signal intensities of the characteristic mass peak, the online partial flux is calculated as follows:

$$J_i(t)=J_i(t=\infty)\times\frac{I_i(t)}{I_i(t=\infty)} \quad (22)$$

where $I_i(t)/I_i(t=\infty)$is the ratio between the electrical signal intensity of the compound *i* in the instant *t* and at the steady state (t=∞). Time-dependent diffusion coefficients, D_i(t) (m^2/s), are calculated in a simplification of Eq. (19), as the ratio c_i^{perm}/H_i is negligible compared to the feed concentration of solute *i* in the bulk feed side, c_i^{feed}:

$$D_i(t)=\frac{J_i(t)}{S_i^L}\times C_{i,feed} \quad (23)$$

Time-dependent diffusivity reflects the evolvement of solute's transport process across the membrane from the first initial instants of permeation, when the membrane contains no permeating species, until the steady state is reached, when the solute-membrane interactions are already well established. Therefore, time-dependent diffusivities may assess potential rearrangements of the membrane structure when permeated by different solutes (especially with affinity to the membrane). Additionally, on-line MS monitoring allows an accurate identification of the commencement of the steady state.

3. Experimental

3.1. PDMS membranes preparation

EL.LR 7660A (component A) elastomer and EL.LR 7660B (component B) curing agent, kindly provided by Wäcker Chemie GmbH (Germany), were used for the preparation of PDMS membranes. According to the supplier's information, component A was a vinyl-methyl-polysiloxane (molecular weight of ca. 40,000 g/mol) containing platinum based catalyst, and component B was a hydrogen functional crosslinker. Hexane, of analytical grade, was purchased from Avantor Performance Materials Poland S.A. (Gliwice, Poland).

A solution containing 20 wt% of component A in n-hexane was prepared and subsequently crosslinking component B was added to the solution to obtain the desired B: A ratio (2:10 or 1:10). The solution was mixed on a magnetic stirrer overnight. Next, a weighted amount of the solution was spread out onto a previously levelled stainless steel mould (round of 125 mm diameter or rectangular of 360×65 mm). The mould was left overnight for evaporation of the solvent (hexane). Subsequently the mould with the membrane was placed in an oven at defined temperature for a given period of time to complete membrane crosslinking. Afterwards, the crosslinked membrane was peeled off from the mould. Detailed information of membrane preparation conditions and membranes properties is summarised in Table 1.

The thicknesses of the PDMS membranes obtained were high, in order to avoid the influence of the feed boundary layer, and consequently feed polarisation effects, during the transport of the solutes across these membranes [15]. In that way, a better understanding of the transport mechanisms of a solute across these membranes is simpler to carry out.

3.2. Compounds

Feed solutions used in this work were prepared using the following compounds: ethyl acetate – EtAc (99.5%, Merck, USA), hexyl acetate – HxAc (99%, Sigma-Aldrich, USA) and deionised water. Ethanol (99.8%, VWR, Germany) was also used for the homogenisation of the two phases in the permeate before the Gas Chromatography analysis.

3.3. Experimental set-up

The pervaporation-condensation system was combined to the on-line mass spectrometry monitoring tool as shown in Fig. 2.

The experimental set-up is composed of a flat membrane stainless steel test cell, which provides a radial flow, and a U-shaped glass trap, immersed in liquid nitrogen, to condense all the permeate vapours. The feed solution was placed in a jacketed vessel in which the temperature of water was controlled by a thermostated bath (model CW 05 G, JeioTech, Korea). The pervaporation module and the permeate circuit was covered with a heating tape connected to a temperature controller (CB100, from RKC Instruments Inc., Japan) to maintain a temperature of 40 °C. To assure vacuum conditions in the downstream circuit, a rotary vane pump (DUO 2.5, Pfeiffer Vacuum, Germany) was used. The pressure was measured using a pressure gauge consisting of a capacitance manometer, model 600 Barocel, and a transducer power supply model 1575 (BOC Edwards, UK). The pervaporation circuit was connected to the MS by a splitting system consisted of a sapphire needle valve heated at 60 °C to avoid vapour condensation in this line.

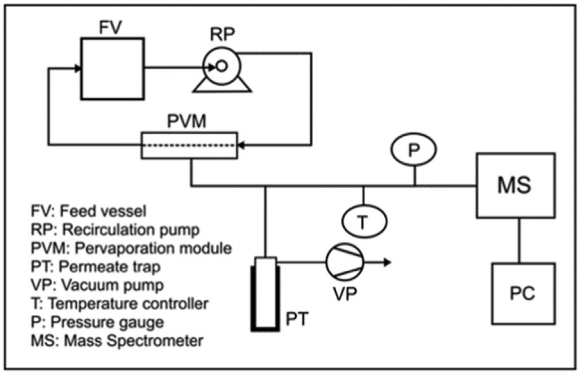

Fig. 2. Experimental pervaporation setup with online monitoring of the permeate stream through Mass Spectrometry (MS).

The mass spectrometer (Prisma Plus QMG 220 M2, Pfeiffer Vacuum, Germany) was used with an axial beam ion source, emission current 1 mA, electron energy 70 eV, single quadrupole, secondary electron multiplier SEM detection.

3.4. Operating conditions

Various feed solution compositions were used; i.e. 2 wt%, 0.5 wt% and 300 ppm of ethyl acetate in deionised water and 300 ppm of hexyl acetate in deionised water. An appropriate amount of solvent was added to the feed tank (in the beginning of the experiments) after four hours of membrane conditioning in the contact with pure solvent. This moment was regarded as the beginning of experiments. The volume of the feed tank was equal to 1 and 11 L in the case of ethyl acetate and hexyl acetate, respectively. These volumes were kept constant in a closed vessel using a reduced headspace. The feed Reynolds was maintained constant at 430 [14]. The temperature of the feed vessel and the permeate circuit was kept at 40 °C.

3.5. Sorption experiments

Sorption experiments of aroma compounds in the PDMS membrane material were conducted at 40 °C with various binary mixtures of ethyl acetate (EtAc) and hexyl acetate (HxAc) in water with concentration similar to those in the pervaporation experiments (2 wt% EtAc, 0.5 wt% EtAc and 300 ppm EtAc in water and 300 ppm HxAc in water). Small pieces of PDMS material were placed in contact with the solution in a mass ratio of solution to material of 4:1, in GC vials of 10 mL also used for headspace analysis in order to assure a closed system. The vials were stirred in a mixer under controlled temperature during 48 h to ensure a system at equilibrium conditions at the end of each sorption experiment. The concentrations of aroma compounds at the beginning and at the end of each sorption experiment were obtained by Gas Chromatography GC (CP-3800, Varian, USA) connected to an automatic sampler (Combi PAL, CT Analytics, Switzerland). The static headspace sampling technique used is reported in [19]. The GC column and method used are reported in [20].

3.6. Mass spectrometry monitoring

A mass spectrometer detects compounds according to their specific

Table 1
Conditions of PDMS membranes preparation and resulting chosen properties.

Membrane	Crosslinking agent/PDMS weight ratio (-)	Crosslinking temperature (°C)	Crosslinking time (h)	Water contact angle (deg.)	Membrane thickness (μm)
PDMS 25	1:10	70	2	103 ± 3	269 ± 66
PDMS 50	1:5	70	2	104 ± 1	330 ± 62

mass to charge ratio (m/z) and intensity of electric signal, providing a characteristic mass spectra of a specific compound. To detect all mass fragments (m/z) of a defined compound, the mass spectra are acquired in the scan mode and the characteristic mass peaks are chosen. MS data is shown in a multiple ion detector (MID) mode with the electric signal chosen for each compound as explained in [11]. The selected mass fragments monitored were: m/z 18 for water, m/z 43 for ethyl acetate and m/z 43 also for hexyl acetate (ethyl acetate and hexyl acetate were not present simultaneously in the samples). The calibration procedure used is described in detail elsewhere [12]. Briefly, it converts the MS intensity of each individual utilised compound into its corresponding pressure assuring that each compound under study is the only specie in the circuit. The temperature is maintained constant as in the pervaporation experiments and measured and controlled with a temperature controller (CB100, from RKC Instruments Inc., Japan) connected to a heating tape in the circuit. This calibration procedure can be performed within a wide range of partial pressures.

4. Results and Discussion

Since this study aims at evidencing and understanding the role of solute-membrane interactions in the transport of solvent and solute through dense membranes during a pervaporation process, it was necessary, as the first step, to assure that the behaviour observed could be associated to the membrane itself and not to the external mass transfer phenomena occurring in the feed phase boundary layer.

4.1. Effect of feed boundary layer

Experiments were performed with the membrane with the higher degree of crosslinking, PDMS 50. For the overall transport of 300 ppm of ethyl acetate and 300 ppm of hexyl acetate in aqueous solution, and as explain in detail in Section 2.1, the overall mass transfer resistance $1/k_{i,\ ov}$ (s/m), the feed boundary layer resistance $1/k_{i,\ bl}$ (s/m), the membrane mass transfer resistance $1/k_{i,m}S_i^L$(s/m) and the feed boundary layer thickness z_{bl} (m) were calculated respectively by Eqs. (3), (5), (4) and (6). The obtained values are listed in Table 2.

It was found that the membrane mass transfer resistance is two orders of magnitude higher than the feed boundary layer resistance (Table 2). Therefore, it may be concluded that most of the resistance during the overall transport of the solute occurs during transport across the membrane. This result was expected for ethyl acetate since its sorption coefficient is relatively low and the fluid dynamic conditions used in the feed compartment of the pervaporation cell are good enough to minimise concentration polarisation effects [14], but concentration polarisation effects could be expected for hexyl acetate, which exhibits a much higher affinity towards the membrane. In order to avoid this effect we decided to use thick PDMS membranes (approximately 330 μm). As reported in Baker et al. [15], the permeation of volatile organic compounds is controlled by the membrane for thick silicone rubber membranes (more than 20 μm) and this phenomenon dominates over the stagnant boundary layer. In this case, the thickness of the membrane PDMS 50 selected in this work was similar to the calculated thicknesses of the feed boundary layer (Table 2). For a similar thickness, the diffusion of the solute in the liquid (i.e. in the boundary layer) is faster than its diffusion across the membrane. Therefore, it can be assumed that in all studies accomplished and discussed in this work, the overall mass transfer resistance is controlled by the membrane mass transfer resistance. From Table 2 it can be observed that the boundary layer thickness was similar for both solutes, since the fluid dynamics in the pervaporation cell was the same, and this data is in a good agreement with results reported in literature [21].

Table 2
Transport parameters determined for 300 ppm ethyl acetate (EtAc) and 300 ppm hexyl acetate (HxAc) during pervaporative separation with PDMS 50 membrane.

PDMS 50 (δ=330 μm)		
EtAc		HxAc
J_i (10^{-10} m s^{-1})	0.14	0.38
$1/k_{i,\ ov}$ (10^{-4} m s^{-1})	426.2	98.3
$1/k_{i,\ bl}$ (10^{-4} m s^{-1})	1.2	1.5
$1/k_{i,m}$ S_i (10^{-4} m s^{-1})	425.0	96.8
z_{bl} (μm)	369.3	327.9
$D_{i\text{-}j}$ (10–8 m^2 s^{-1})	3.1	2.1

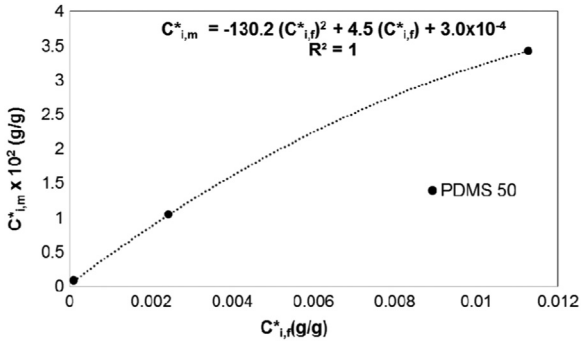

Fig. 3. Ethyl acetate concentration in the membrane as a function of its concentration in solution, at 40 °C. Symbols correspond to experimental data obtained for PDMS 50.

4.2. Determination of sorption experiments

The knowledge of sorption coefficient is essential to calculate the diffusivities of the solutes across the membrane. Therefore, sorption experiments were performed under the same conditions used in pervaporation experiments. Fig. 3 represents the sorption isotherm of ethyl acetate in contact with the PDMS 50 membrane at 40 °C, with $C^*_{i,m}$ and $C^*_{i,f}$ correspond to equilibrium concentrations (in weight fractions units), respectively in the membrane and in the liquid, obtained by gas chromatography. The sorption coefficient of ethyl acetate in PDMS was calculated using Eq. (24):

$$S_i = \frac{C^*_{i,m}}{C^*_{i,f}} \tag{24}$$

The values of the sorption coefficient of ethyl acetate were found to vary with its concentration and may be easily obtained as the slope of the equilibrium isotherm for each value of liquid composition (Fig. 3). The concentration of the solute in the boundary layer next to the membrane was considered to be the same as the bulk concentration of the solute, since feed-side concentration polarisation effects were found to be not relevant in the systems under study, as proven in the previous section [15]. As expected, the sorption coefficient of ethyl acetate in PDMS 50 varied with the concentration of the solute in the liquid phase, in particular in the region of higher solute concentration (usually a linear relationship is observed for very diluted systems). Due to the similar characteristics for both membranes (as the transport results shows in the transient transport section), the sorption isotherm of ethyl acetate was considered to be identical for the PDMS 25 membrane.

The sorption coefficient of hexyl acetate (at the concentration of 300 ppm in aqueous solution) in PDMS 50 was calculated directly through Eq. (23). Considering that hexyl acetate was extremely diluted in the aqueous solution (300 ppm in the feed solution), the sorption coefficient of hexyl acetate was assumed to be constant in the range of concentrations between infinite dilution and 300 ppm. Table 3 summarises the experimental sorption coefficients of ethyl acetate and hexyl acetate in the PDMS 50 membrane, for different feed concentrations.

The hexyl acetate sorption coefficient in PDMS 50 was found to be

Table 3
Sorption coefficient S_i^L of ethyl acetate (EtAc) and hexyl acetate (HxAc) in contact with PDMS 50 membrane.

Feed solution	Sorption coefficient S_i^L (-)
20 000 ppm (2.0 wt%) EtAc	2.0
5 000 ppm (0.5 wt%) EtAc	3.9
300 ppm EtAc	5.4
300 ppm HxAc	530

two orders of magnitude higher than that for ethyl acetate (Table 3), indicating an extremely high affinity of hexyl acetate to the membrane material. A similar behaviour was observed for the sorption coefficients of hexyl acetate and ethyl acetate in poly(octylmethylsiloxane) POMS material [22].

4.3. Permeation experiments

4.3.1. Steady state transport

The first objective of this study was to assess the impact of solute partitioning and penetration in the membrane material on the transport of solvent. Such impact is expected because, as the solute solubilises within the membrane material, it promotes changes on the internal arrangement of the polymeric chains. This rearrangement, required to accommodate the new entity, may lead to a process of membrane fluidification which impacts the transport of all chemical species present in solution.

Fig. 4 shows the solvent flux (water) through different membrane materials, when using different concentrations of ethyl acetate in the feed compartment (300 ppm, 0.5 wt% and 2 wt% of ethyl acetate in water) and different solutes (ethyl and hexyl acetate).

Fig. 4(a) shows, in first place, the extremely high impact of solute (ethyl acetate) concentration on the flux of solvent across PDMS membranes, irrespectively from their degree of crosslinking. This impact is impressive and translates how the penetration of the solute inside the membrane, even for a solute with a relatively modest sorption coefficient for PDMS, promotes an internal rearrangement of the polymeric material that leads to a much faster diffusion of water molecules across the membrane. Also, from Fig. 4(a) we may conclude that the two membranes prepared do not differ much from each other. Actually, it is possible to observe a slightly lower water flux through the membrane prepared with a higher degree of crosslinking, PDMS 50, but this effect is not particularly significant.

The minor effect of the degree of crosslinking is also noticeable in Fig. 4(b) where the flux of water is slightly lower for the PDMS 50 membrane in the whole range of solute concentration. Fig. 4(b) emphasises again how important is the influence of solute concentration on the flux of solvent. The results obtained represent a 10 fold increase in water flux, if we compare the situation of pure water with the processing of an aqueous solution with 2 wt% of ethyl acetate. As discussed above, solute solubilisation in the membrane material involves the need for accommodating its molecules within the polymeric structure, inducing a significant fluidification effect, with impact on the diffusion of labile water molecules.

This effect is even more pronounced when comparing the water flux for two different aqueous solutions, one with ethyl acetate and the other with hexyl acetate, at the same concentration of 300 ppm. Hexyl acetate presence leads to a higher water flux (80% increase), which reflects a higher degree of membrane rearrangement and fluidification, which is naturally explained by the extremely high sorption coefficient of hexyl acetate towards the membrane. This means that the local concentration within the membrane is much higher for hexyl acetate. This feature, together with the fact that hexyl acetate is a more bulky solute, which accommodation induces a higher degree of rearrangement, explains the behaviour observed.

Table 4 summarises the impact of solute concentration on its own transport across membranes with a different degree of crosslinking. Solute partial fluxes (calculated from the total fluxes and permeate composition), permeabilities, diffusion coefficients, selectivities and enrichment factors, obtained from the steady state data, are listed in this table for ethyl acetate/water and hexyl acetate/water systems.

The first observation is that there is a minor effect of the degree of crosslinking on the transport of solutes. For the same ethyl acetate concentration in the feed solution, the crosslinking ratio does not seem to affect significantly the membrane transport properties since solute partial flux, permeability and diffusion coefficients are similar. These results are comparable with those obtained by Nguyen et al. [23] where the diffusion coefficients found are negligibly affected by different

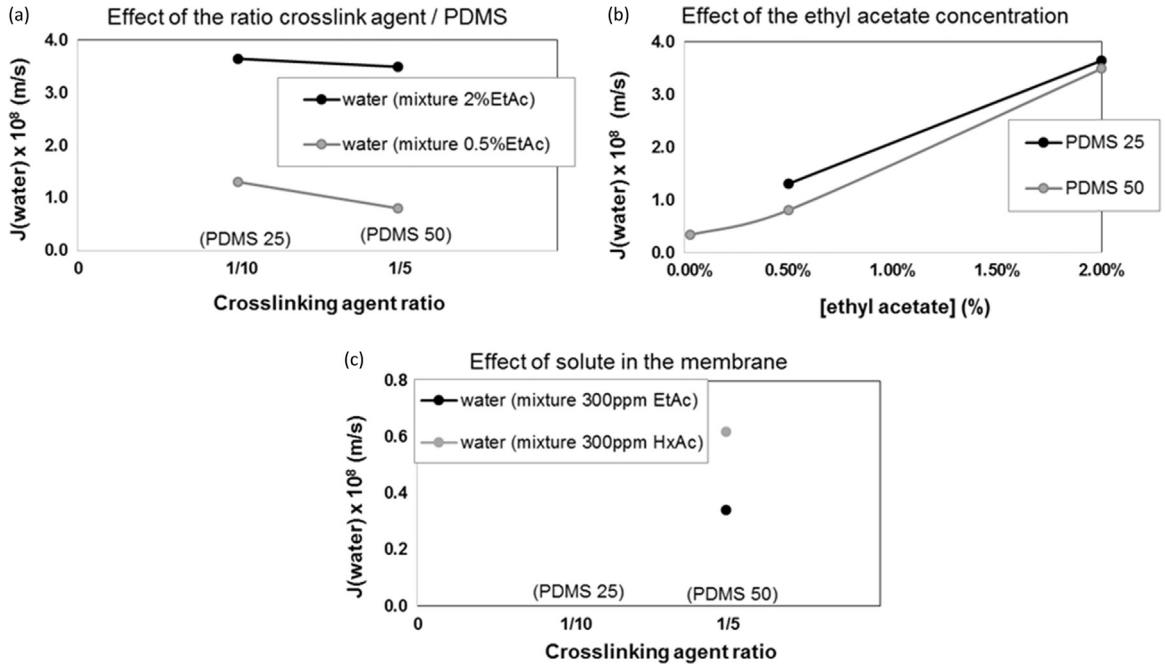

Fig. 4. Flux of water through PDMS membranes: (a) membranes prepared with different crosslinking degree; (b) effect of solute (ethyl acetate) concentration in the feed solution; (c) effect of solute type (ethyl acetate and hexyl acetate).

Table 4
Impact of solute concentration on its own transport across PDMS membranes, for aqueous solutions with 2 wt%, 0.5 wt% and 300 ppm of ethyl acetate and 300 ppm of hexyl acetate in water at 40 °C.

Membrane	Feed composition	J_i (10^{-11} m s^{-1})	P_i (10^{-10} m^2 s^{-1})	D_i (10^{-12} m^2 s^{-1})	Selectivity α_{i-j} (-)	Enrichment EF (-)
PDMS 25	2.0 wt% EtAc	650.0 ± 7.0	4.3 ± 0.0(2)	220.0 ± 2.1	43.9 ± 0.2	7.8 ± 0.0(4)
	0.5 wt% EtAc	64.0 ± 0.8	1.7 ± 0.0(2)	40.0 ± 0.6	47.3 ± 0.6	9.3 ± 0.0
PDMS 50	2.0 wt% EtAc	603.0 ± 4.0	5.2 ± 0.0(3)	260.0 ± 1.6	43.7 ± 0.3	7.8 ± 0.0
	0.5 wt% EtAc	53.0 ± 0.4	1.8 ± 0.0(1)	50.0 ± 0.3	63.9 ± 0.5	12.3 ± 0.0(8)
	300 ppm EtAc	1.4 ± 0.0(4)	0.8 ± 0.1	10.0 ± 0.3	68.9 ± 1.7	14.0 ± 0.3
	300 ppm HxAc	3.8 ± 0.0(4)	3.5 ± 0.0(1)	0.7 ± 0.0(1)	163.9 ± 2.2	20.3 ± 0.1

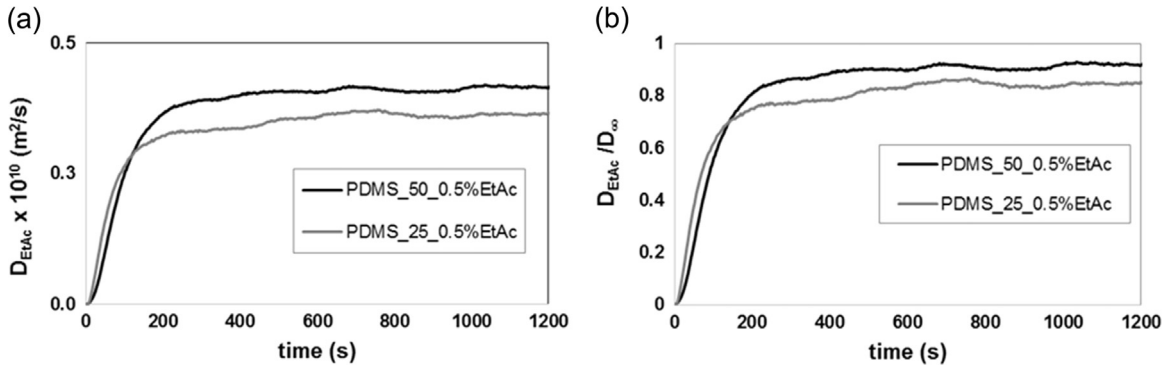

Fig. 5. (a) Ethyl acetate diffusion coefficient and (b) normalised ethyl acetate diffusion coefficient for PDMS 25 and PDMS 50, using a feed aqueous solution of ethyl acetate with a concentration of 0.5 wt% at 40 °C. Data obtained by on-line mass spectrometry.

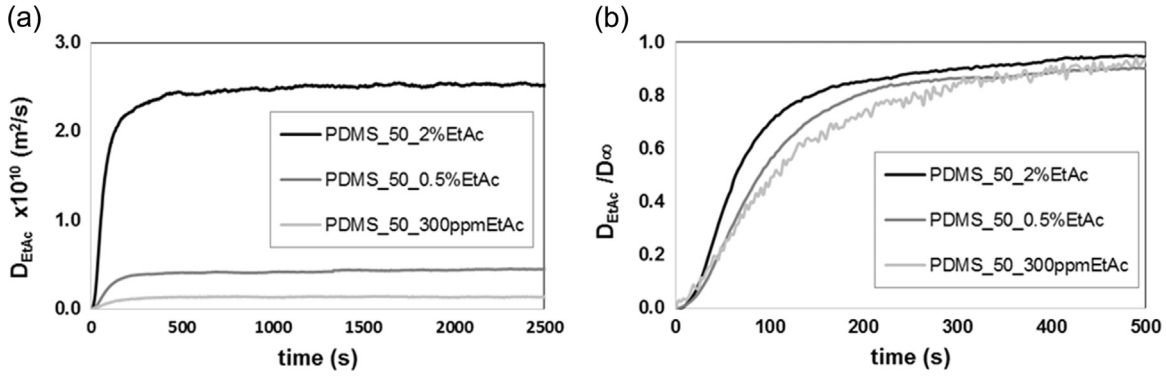

Fig. 6. Comparison of (a) evolvement of solute diffusion coefficient and (b) evolvement of normalised diffusion coefficient of ethyl acetate in PDMS 50, when using aqueous solutions 2 wt%, 0.5 wt% and 300 ppm of ethyl acetate, at 40 °C.

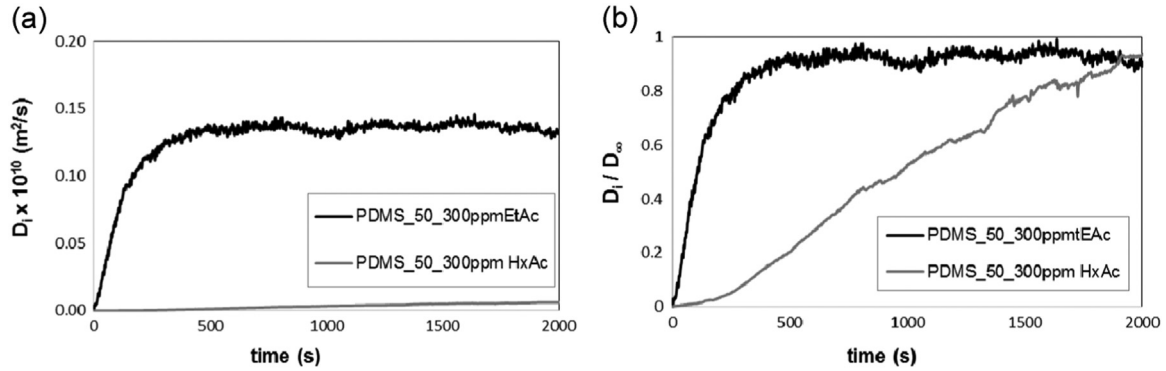

Fig. 7. Evolvement of (a) the diffusion coefficient for ethyl acetate and hexyl acetate and (b) normalised diffusion coefficient, through a PDMS 50 membrane, for a concentration of solute of 300 ppm in water, at 40 °C.

crosslinked PDMS membranes. On the other hand, an increase of solute concentration leads to an increase of solute flux, permeability and diffusivity, evidencing that membrane fluidification induced by the partitioning of solute impacts strongly the transport of solute.

When comparing solutes with different affinity towards the membrane (ethyl acetate and hexyl acetate), a significantly higher solute flux, permeability and selectivity were found for hexyl acetate. This behaviour is explained by the much higher affinity and interaction of

hexyl acetate with the membrane material, which induces a stronger rearrangement/fluidification of the membrane.

4.3.2. Transient transport studies

Transient transport studies were performed with the objective of obtaining information about transport behaviour in the initial period of operation, when the membrane is adjusting to the solubilisation and interaction of solute within its material.

4.3.2.1. Effect of degree of crosslinking. Pervaporation experiments were performed using on-line mass spectrometry monitoring. These experiments were accomplished for the membranes prepared with different crosslinking ratio, as shown in Table 1, in order to evaluate the impact of this parameter in the performance of the pervaporation process. From Fig. 5a and b, similar behaviours were observed for the diffusion coefficients of ethyl acetate, and their evolvement along the time, for both membranes under study. Diffusion coefficients of ethyl acetate through both membranes, crosslinked at different degrees, are similar suggesting that the membranes' behaviour and their potential rearrangement induced by solute solubilisation is also similar in both cases.

4.3.2.2. Effect of solute concentration. Different concentrations of the same solute were also tested using the PDMS 50 membrane, in order to evaluate the impact of this parameter on the membrane behaviour and, consequently, on solute transport. As shown in Fig. 6, higher ethyl acetate concentrations led to higher solute diffusion coefficients in both membranes. This result was expected since higher local solute concentrations within the membrane lead to higher solute-membrane interactions, which determine a deeper degree of membrane fluidification with the corresponding impact in terms of solute diffusion. This is the reason why the solute diffusion coefficient progressively increases along time, translating the progressive modification of the membrane. It is also interesting to notice (Fig. 6b) that, when the concentration of solute is lower, the process of membrane rearrangement/increase of normalised solute diffusion coefficient ($D(t)/D_{(t=\infty)}$) is slower, taking longer to reach a steady-state condition.

4.3.2.3. Effect of solute nature. Ethyl acetate and hexyl acetate were selected to perform studies aiming to understand the impact of the solute type on the membrane fluidification and, ultimately, solute diffusion. The pervaporation experiments were performed exactly in the same conditions for both solutes.

These two solutes were selected because chemically they are both esters but hexyl acetate has a much higher affinity towards the PDMS membrane than ethyl acetate, quantified by their sorption coefficients in PDMS (two orders of magnitude higher). This higher affinity translates into a much higher local concentration within the membrane, leading to a higher membrane fluidification. Nevertheless, the absolute values of the diffusion coefficient of hexyl acetate were lower than the values for ethyl acetate (Fig. 7a), because this solute has a significantly higher molecular mass and, being bulkier, its diffusion within the polymeric membrane structure is significantly more hindered.

The normalised diffusion coefficients (Fig. 7b) clearly show a great difference between the permeation of the two solutes. Hexyl acetate permeation reaches steady-state during a much slower process, which is explained by the more extensive rearrangement induced within the membrane structure, as discussed (in the Section 4.3.1).

5. Conclusions

In this work, organophilic sorption and pervaporation studies were carried out in order to assess the impact of selected parameters involved in the permeation of organic compounds from dilute aqueous media under transient and steady states. The thickness of prepared membranes was high, which allowed to neglect the influence of concentration polarisation on the transport.

The main results that should be retained are:

- The Mass Spectrometry technique used proves to be a very powerful technique that allows for obtaining high quality data for studying membrane transport phenomena, in particular when information from transient regime is required.
- Solute solubilisation within the membrane polymer matrix induces internal rearrangements that impact not only on the transport of solutes themselves, but also on the transport of solvent. It was found that flux of solvent increases substantially with an increase of solute concentration in feed.
- Solute transport evolves during the transient period during which the impact of solute solubilisation translates into a rearrangement of the membrane polymeric structure. This impact is more relevant for bulky solutes with a high partitioning affinity to induce strong membrane rearrangement;
- The approach discussed in this work is very useful for further research on solute transport (not only in pervaporation studies but also vapour permeation and gas permeation [24], which can be easily monitored by MS) and design of novel membrane materials [25].

As a future work, the rearrangement of the membrane polymeric structure during solute transport might be monitoring by PALS Positron Annihilation Lifetime Spectroscopy, in order to complement the data obtained from the MS.

Acknowledgments

The authors would like to acknowledge the Fundação para a Ciência e Tecologia, Portugal for the Ph.D grant of Sofia Fraga (SFR/BD/81814/2011) and the Post-Doctoral Fellow Grant of Carla Brazinha (SFR/BD/79533/2011).

This work was supported by the grant N N209 761240, funded by National Science Centre Poland. Erasmus LLP mobility grant, which enabled research internship of Anna Kujawska (Rozicka) at the Universidade Nova de Lisboa in Lisbon, Portugal, is also acknowledged.

References

[1] Z. Wang, A.A. Volinsky, N.G. Gallant, Crosslinking effect on polydimetilsyloxane elastic modulus measured by custom-built compression instrument, J. Appl. Polym. Sci. 41050 (2014) 1–4.
[2] Q.T. Nguyen, Z. Bendjama, R. Clément, Z. Ping, Poly(dimethylsiloxane) crosslinked in different conditions. Part I. Sorption properties in water-ethyl acetate mixture, Phys. Chem. Chem. Phys. 1 (1999) 2761–2766.
[3] J. Kujawski, A. Rozicka, M. Bryjak, W. Kujawski, Pervorative removal of acetone, butanol and ethanol from binary and multicomponent aqueous mixture, Sep. Purif. Technol. 132 (2014) 422–429.
[4] T.A. Weschenfelder, P. Lantin, M. Caldeira Viegas, F. de Castilhos, A. de Paula Scheer, Concentration of aroma compounds from an industrial solution of soluble coffee by pervaporation process, J. Food Eng. 159 (2015) 57–65.
[5] M. She, S.-T. Hwang, Concentration of dilute flavour compounds by pervaporation: permeate pressure effect and boundary layer resistance mode, J. Membr. Sci. 234 (2004) 193–202.
[6] A. Hasanoglu, Y. Salt, S. Keleser, S. Ozkan, S. Dinçer, Pervaporation separation of ethyl-acetate- ethanol binary mixtures using polydimethylsiloxane membrane, J. Membr. Sci. 234 (2004) 193–202.
[7] J.G. Wijmans, R.W. Baker, The solution-diffusion model: a review, J. Membr. Sci. 107 (1995) 1–21.
[8] G.M. Shi, H. Chen, J.C. Jean, T.S. Chung, Sorption, swelling and free volume of polibenzimidazole (PBI) and PBI/zeolitic imidazolate framework (ZIF-8) nano-

composite membranes for pervaporatio, Polymer 54 (2013) 774–783.
[9] K. Tanaka, H. Kita, K.I. Okamoto, R.D. Noble, J.L. Falconer, Isotopic-transient permeation measurements in steady-state pervaporation through polymeric membrane, J. Membr. Sci. 197 (2002) 173–183.
[10] S.C. Fraga, L. Trabucho, C. Brazinha, J.G. Crespo, Characterisation and modelling of transient transport through dense membranes using on-line mass spectrometr, J. Membr. Sci. 479 (2015) 213–222.
[11] T. Schäfer, J. Vital, J.G. Crespo, Coupled pervaporation/mass spectrometry for investigating membrane mass transport phenomena, J. Membr. Sci. 241 (2004) 197–205.
[12] C. Brazinha, A.P. Fonseca, O.M.N.D. Teodoro, J.G. Crespo, On-line and real time monitoring of organophilic pervaporation by spectrometr, J. Membr. Sci. 347 (2010) 83–92.
[13] Y. Hasegawa, K. Kimura, Y. Nemoto, T. Nagase, Y. Kiyozumi, T. Nishide, F. Mizukami, Teal-time monitoring of permeation properties through polycrystalline MFI-type zeolite membranes during pervaporation using mass spectrometr, Sep. Purif. Technol. 58 (2008) 386–392.
[14] T. Schäfer, J.G. Crespo, Study and optimization of the hydrodynamic upstream conditions during recovery of a complex aroma profile by pervaporatio, J. Membr. Sci. 301 (2007) 46–56.
[15] R.W. Baker, J.G. Wijmans, A.L. Athayde, R. Daniels, J.H. Ly, M. Le, The effect of concentration polarization on the separation of volatile organic compounds from water by pervaporatio, J. Membr. Sci. 137 (1997) 159–172.
[16] A.M. Urtiaga, E.D. Gorri, I. Ortiz, Modelling the concentration-polarization effects in a pervaporation cell with radial flo, Sep. Purif. Technol. 17 (1999) 41–51.
[17] C.R. Wilke, P. Chang, Correlation of diffusion coefficients in dilute solution, AIChE J. 1 (2) (1955) 264–270.
[18] R.W. Baker, J.G. Wijmans, Y. Huang, Permeability, permeance and selectivity: a preferred way of reporting pervaporation performance date, J. Membr. Sci. 348 (2010) 346–352.
[19] C. Brazinha, V.D. Alves, R.M.C. Viegas, J.G. Crespo, Aroma recovery by integration of sweeping gas pervaporation and liquid absorption in membrane contactor, Sep. Purif. Technol. 70 (2009) 103–111.
[20] C. Brazinha, J.G. Crespo, Aroma recovery from hydro alcoholic solutions by organophilic pervaporation: modelling of fractionation by condensation, J. Membr. Sci. 341 (2009) 109–121.
[21] M.J. She, S.T. Hwang, Concentration of dilute flavor compounds by pervaporation: permeation pressure effect and boundary layer resistance modeling, J. Membr. Sci. 236 (2004) 193–202.
[22] T. Schäfer, A. Heintz, J.G. Crespo, Sorption of aroma compounds in poly(octylmethylsiloxane) (POMS), J. Membr. Sci. 254 (2005) 259–265.
[23] Q.T. Nguyen, Z. Bendjama, R. Clément, Z. Ping, Poly(dimethylsiloxane) crosslinked in different conditions. Part II. Pervaporation of water-ethyl acetate mixture, Phys. Chem. Chem. Phys. 2 (2000) 395–400.
[24] K. Pilnacek, J.C. Jansen, P. Bernardo, G. Clarizia, F. Bazzarelli, F. Tasselli, Determination of mixed gas permeability of high free volume polymers using direct mass spectrometric analysis of the gas composition, Proc. Eng. 44 (2012) 1027–1029.
[25] C.R. Mason, L. Maynard-Atem, K.W.J. Heard, B. Satilmis, P.M. Budd, K. Friess, M. Lanc, P. Bernardo, G. Clarizia, J.C. Jansen, Enhancement of CO_2 Affinity in a Polymer of Intrinsic Microporosity by Amine Modification, Macromol 47 (2014), 2014, pp. 1021–1029.

View publication stats